

What do tropical cryptogams reveal? Strong genetic structure in Amazonian bryophytes

Alice Ledent^{1*} , Jérémy Gauthier^{2*} , Martinha Pereira³, Rick Overson⁴, Benjamin Laenen⁵, Patrick Mardulyn⁶ , S. Robbert Gradstein⁷ , Myriam de Haan⁸, Petra Ballings⁸, Iris Van der Beeten⁸, Charles E. Zartman²  and Alain Vanderpoorten¹ 

¹Institute of Botany, University of Liège, B22 Sart Tilman, Liège 4000, Belgium; ²Muséum d'Histoire Naturelle, route de Malagnou 1, Genève 1208, Switzerland; ³Department of Biodiversity, National Institute for Amazonian Research, Petrópolis, CEP 69060-001, Manaus, Amazonas, Brazil; ⁴Global Institute of Sustainability, Arizona State University, Tempe, AZ 85281, USA; ⁵Department of Ecology, Environment and Plant Sciences, Science for Life laboratory, Stockholm University, Stockholm 106 91, Sweden; ⁶Evolutionary Biology and Ecology, Université Libre de Bruxelles, Brussels 1050, Belgium; ⁷Institut de Systématique, Evolution, Biodiversité (ISYEB), Muséum national d'Histoire naturelle, CNRS, EPHE, Sorbonne Université, CP 39, 57 rue Cuvier, Paris F-75005, France; ⁸Research Department, Meise Botanic Garden, Meise 1860, Belgium

Summary

Author for correspondence:
Alain Vanderpoorten
Tel: +32 43663842
Email: a.vanderpoorten@uliege.be

Received: 31 March 2020
Accepted: 25 May 2020

New Phytologist (2020)
doi: 10.1111/nph.16720

Key words: Amazonia, bryophytes, isolation-by-distance, restriction site-associated DNA sequencing (RADseq), spatial genetic structure, tropical rainforest.

- Lowland tropical bryophytes have been perceived as excellent dispersers. In such groups, the inverse isolation hypothesis proposes that spatial genetic structure is erased beyond the limits of short-distance dispersal. Here, we determine the influence of environmental variation and geographic barriers on the spatial genetic structure of a widely dispersed and phylogenetically independent sample of Amazonian bryophytes.
- Single nucleotide polymorphism data were produced from a restriction site-associated DNA sequencing protocol for 10 species and analyzed through F-statistics and Mantel tests.
- Neither isolation-by-environment nor the impact of geographic barriers were recovered from the analyses. However, significant isolation-by-distance patterns were observed for 8 out of the 10 investigated species beyond the scale of short-distance dispersal (> 1 km), offering evidence contrary to the inverse isolation hypothesis.
- Despite a cadre of life-history traits and distributional patterns suggesting that tropical bryophytes are highly vagile, our analyses reveal spatial genetic structures comparable to those documented for angiosperms, whose diaspores are orders of magnitude larger. Dispersal limitation for tropical bryophytes flies in the face of traditional assumptions regarding their dispersal potential, and suggests that the plight of this component of cryptic biodiversity is more dire than previously considered in light of accelerated forest fragmentation in the Amazon.

Introduction

The extraordinary diversity in Amazonia, which hosts the richest terrestrial biodiversity on Earth (Cheng *et al.*, 2013), results from long and complex interactions between geologic, climatic and ecological processes (Hoorn & Wesselingh, 2010; Smith *et al.*, 2014). By far the most impressive feature of the geography of the Amazon basin is the presence of large rivers such as the Amazon and the Rio Negro, the first two most important rivers in terms of annual discharge in the world. Such rivers may, as Wallace (1852) already hypothesized, act as barriers to gene flow between populations inhabiting opposite river banks, thus promoting speciation. This hypothesis has subsequently been supported by molecular evidence in a wide range of organisms including vertebrates (see Ortiz *et al.*, 2018 for review) and dominant, canopy-

emergent trees (Nazareno *et al.*, 2019), but questioned in others characterized by higher dispersal capacities (Santorelli *et al.*, 2018), whose distributions are expected to be more strongly associated with local environmental conditions rather than with the presence of barriers or geographic distance (isolation-by-distance, IBD; Dambros *et al.*, 2017). In higher plants for instance, the gradient hypothesis proposes that strong environmental gradients, like white-sand forests adjacent to other forests, on relatively more nutrient-rich soils, called 'terra firme', promote isolation by environment (IBE; Wang & Bradburd, 2014). Mounting evidence for weak spatial genetic structures in flying or wind-dispersed organisms such as birds, butterflies and vascular plants, has, however, escalated the debate as to whether geographic or ecological barriers are the major barriers to dispersal processes (Dambros *et al.*, 2017; Santorelli *et al.*, 2018).

Among land plants, high dispersal capacities and 'all-purpose' genotypes typically characterize bryophytes. Experimental

*These authors contributed equally to this work.

work suggests that, in contrast to the vast majority of angiosperms, bryophytes do not tend to develop ecotypes, but rather display an inherent broad ability to cope with environmental variation (Shaw, 1992). Bryophytes, like all cryptogams, produce extremely small diaspores and as a result are considered excellent dispersers due to their capacity for exceptionally long-distance anemochory (Patiño & Vanderpoorten, 2018). Schuster (1983) specifically considered lowland tropical bryophyte communities as a 'monotonous assemblage of highly dispersive species', and in fact, using null model analyses based on metacommunity concepts for Amazonian epiphytic bryophyte communities, Mota de Oliveira & ter Steege (2015) reported a near absence of floristic dissimilarity in relation to geographic distance at the continental scale of the Amazon basin (6 million km²). Experimental studies conducted in temperate regions offer supporting evidence through spore-trapping experiments, demonstrating fat-tailed dispersal kernels (Sundberg, 2005). A decay of the relationship between spore densities and distance from the source was observed beyond 1 km, as if spores, once airborne, could travel across any distance range (Lönnell *et al.*, 2012). In such conditions, an inverse isolation effect, involving a higher genetic diversity of colonizing propagules with increasing isolation, is predicted to develop (Sundberg, 2005; Barbé *et al.*, 2016), thus counteracting differentiation. Consequently, no IBD is expected beyond a distance corresponding to short-distance dispersal events, owing to the well-mixed and diverse propagule pool (Szövényi *et al.*, 2012), a pattern that was precisely recovered in the liverwort *Cheilolejeunea rigidula* at large spatial scales across Amazonia (Mota de Oliveira *et al.*, 2011, but see Campos Salazar, 2016). Evidence for such strong dispersal capacities has substantial conservation consequences because it would suggest that epiphytes maintain dispersal capacities to overcome the rapid fragmentation of the Amazonian rainforest. However, experimental demographic studies of Amazonian epiphylls conversely revealed that immigration rates decrease with forest fragment size (Zartman & Shaw, 2006; Zartman & Nascimento, 2006) and with reductions in neighbourhood densities (Zartman *et al.*, 2012), pointing to fine-scale dispersal limitations, as further evidenced by analyses of spatial genetic structures (Snäll *et al.*, 2004; Hutsemékers *et al.*, 2010, 2013; Korpelainen *et al.*, 2011, 2012, 2013; Holá *et al.*, 2015).

In the present paper, we test the importance of environmental variation, geographic barriers and geographic distance in explaining the spatial genetic structure of Amazonian bryophyte species. Given the tendency of bryophytes to exhibit broadly adapted, 'all-purpose' genotypes we predict that the spatial genetic structure of Amazonian bryophytes is not explained by environmental variation. Furthermore, if, as experimental works suggest, the density of spore deposition becomes distance-independent after a few hundred meters, the inverse isolation hypothesis should apply. Under such a scenario we predict the following: first, geographic barriers do not contribute to the observed spatial genetic structure and, second, any signal of isolation-by-distance is erased beyond the range of short-distance dispersal.

Materials and Methods

Study area and taxonomic sampling

Ten bryophyte species, including four liverworts (*Archilejeunea juliformis* (Nees) Gradst., *Bazzania hookeri* (Lindenb.) Trevis., *Micropterygium trachyphyllum* Reimers, and *Thysananthus amazonicus* (Spruce) Steph.) and six mosses (*Leucobryum martianum* (Hornsch.) Hampe ex Müll. Hal., *Octoblepharum albidum* Hedw., *Octoblepharum pulvinatum* (Dozy & Molke) Mitt., *Syrrhopodon annotinus* W. D. Reese & D. G. Griffin (including *Syrrhopodon simmondsii* Steere as both species behave like one common gene pool, Pereira *et al.*, 2019a), *Syrrhopodon helicophyllum* Mitt., and *Syrrhopodon hornschurchii* Mart.) were used as models. Specimens of these species were sampled within an area of c. 50 000 km² in the Rio Negro basin north of Manaus (Fig. 1; Supporting Information Table S1). Eighteen to 57 specimens were sampled per species in the course of a 30 km transect along the Rio Solimões, a 150 km transect along the Rio Negro up to (and including) Jaú National Park, and a 150 km transect between Manaus, Presidente Figueiredo and Balbina. Our sampling strategy was to collect specimens located > 100 m from each population, as bryophyte colonies are typically clonal (Korpelainen *et al.*, 2013; Mikulaskova *et al.*, 2014; Holá *et al.*, 2015).

Sampling was conducted in the two main forest types of non-flooded tropical lowland rain forests: upland (*terra firme*) and white-sand (*campinarana*) forests. White-sand forests have long been identified as island-like formations (Costa *et al.*, 2019) of the most acidic and nutrient-poor soils known, surrounded by rainforests growing on more typical soils. They have captured the attention of biologists who have hypothesized that they represented laboratories of evolution producing a unique white-sand fauna and flora characterized by unusual structure, function, and species compositions (Fine & Baraloto, 2016). White-sand forests are in fact characterized by much lower basal areas, above-ground biomass, primary productivity, and hence greater light penetration than terra firme forest (Adeney *et al.*, 2016). As a consequence, white-sand forests host characteristic vascular (Adeney *et al.*, 2016) and bryophyte (Benavides *et al.*, 2016; Sierra *et al.*, 2018) floras that are distinct from the flora on other soils even in the immediate vicinity. In the present sample, *B. hookeri*, *T. amazonicus*, *S. annotinus*, and *S. helicophyllum* were, for instance, completely or largely (< 2 specimens) restricted to white-sand forests. Furthermore, white-sand forests host substantially heavier epiphyte loads characterized by different species communities than those of other Amazonian forest types due to narrow host specificity (Cornelissen & ter Steege, 1989; Benavides *et al.*, 2016; Marí *et al.*, 2016). Therefore, although the selected species were either epiphytic (*A. juliformis*, *T. amazonicus*, *S. helicophyllum*, and *S. hornschurchii*), epiphytic or epixylic on dead logs (*B. hookeri*, *M. trachyphyllum*, *L. martianum*, *O. albidum*, *O. pulvinatum*, *S. simmondsii*), or ground-dwelling (*S. annotinus*), the differentiation between terra firme and white-sand forests provided a major habitat differentiation for the three sampled functional groups in the six remaining

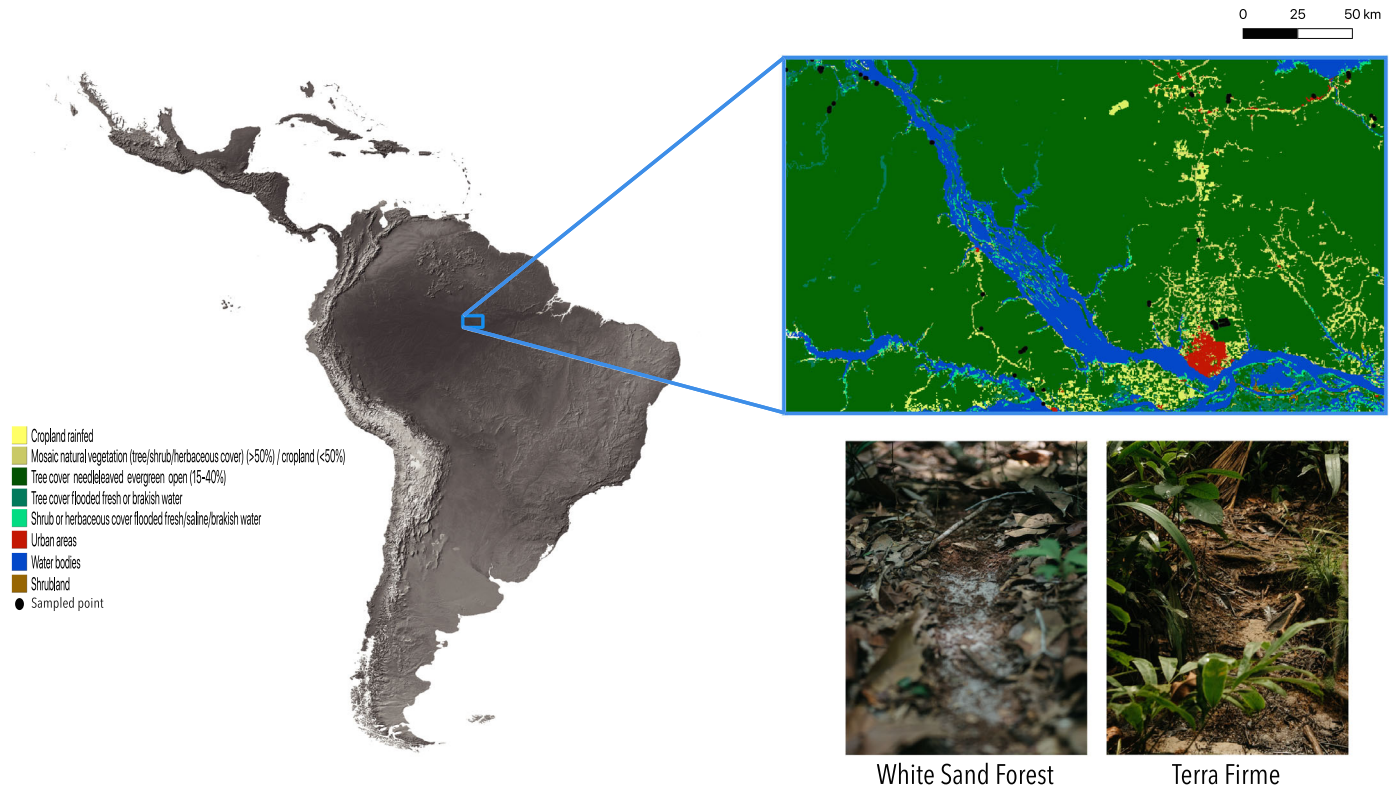


Fig. 1 Study area and sampling design.

species, which occurred in both forest types, and wherein we sought a signature of ecotypification.

Molecular protocols

Samples were frozen in liquid nitrogen for 5 min and DNA was extracted using the DNeasy Plant Mini Kit (Qiagen). SNP libraries were prepared based on a restriction site-associated DNA sequencing (RADseq) protocol modified from the genotyping-by-sequencing (GBS) protocol described by Elshire *et al.* (2011) and starting with the digestion of 100 ng DNA with the enzyme ApeKI. Modifications included the following: (1) a double size selection of DNA fragments of 150–400 bp using SPRI beads (New England Biolabs, Hitchin, UK) to only target fragments, which would efficiently amplify and sequence; (2) an amplification with a Q5 Hot Start High-Fidelity DNA Polymerase (New England Biolabs) to enhance specificity and reduce amplification errors; (3) a scalable complexity reduction using longer 3' primers that cover the entire common adapter, the 3' restriction site and extend 1 or 2 bases into the insert, as implemented in Sonah *et al.* (2013); and (4) a purification of PCR products using AMPure XP beads instead of the QIAquick PCR Purification Kit (Qiagen). We gave each individual a forward and a reverse 4–8 bp barcode (identical, one at the 5' end and one at the 3' end, for paired-end sequencing), such that each individual had a unique barcode for multiplexing. Barcodes were selected from the 384 barcodes specifically designed to be used with ApeKI (<https://www.maizegenetics.net>). The concentration of

PCR products was assessed by fluorometry with the Quant-iT PicoGreen dsDNA Assay Kit (ThermoFisher, Waltham, MA, USA) before multiplexing to ensure the equimolarity of PCR products in final libraries. To detect adaptor contamination (*c.* 128 bp), fragment size distribution was measured for each library with capillary electrophoresis using a QIAxcel (Qiagen). If present, adaptor dimers were removed by selecting fragments of > 150 bp on a polyacrylamide gel. Paired-end sequencing (2 × 75 bp) of the libraries was performed with an NextSeq500 sequencer (Illumina, San Diego, CA, USA) in low-output mode (*i.e.* 130 million reads per lane).

Bioinformatics processing

Sequences of the adaptors at both 3' and 5' ends of each read as well as low-quality sequences (Phred score < 20) at both ends were removed with CUTADAPT v.1.16 (<https://cutadapt.readthedocs.io>). IPYRAD v.0.7.28 (<https://ipyrad.readthedocs.io>) was then used to demultiplex the libraries and to cluster loci using a minimal percentage of identity of 85% within and among individuals. Following Paris *et al.* (2017), we set the minimum number of raw reads required to form an allele (read depth filter) to 3. Due to the haploid condition of the target species, allele clusters with more than one allele per individual were discarded. To avoid linkage among individual SNPs, one SNP per locus was randomly selected.

Following Hodel *et al.* (2017), who recommended that the impact of missing data to a level of 10% of sequenced specimens

per SNP be explored, the data were submitted to a double filtering to take missing data at both the SNP level and the individual level into account using two cutoff values. We first discarded any SNP that was sequenced in either < 10% or < 25% of the individuals, which resulted in two data matrices M1 and M2, respectively. We then filtered-out any individual that was sequenced for < 10% of the SNPs. Therefore, because M1 matrices include many more SNPs than M2, M1 matrices tended to include a lower number of specimens than M2 matrices. We finally computed the percentage of missing data after this double-filtering process for each matrix (Table 1).

To address the issue of the low read-depth, and hence, high missing data rates, we performed a second series of analyses specifically designed for low read-depth GBS and RADseq data. Reads from each sample were mapped on loci resulting from IPYRAD analyses using BWA ALN (Li & Durbin, 2009). Subsequent analyses were performed using ANGSD, allowing the use of genotype likelihoods instead of genotype calls (Korneliussen *et al.*, 2014). Working directly on genotype likelihoods facilitates the incorporation of statistical uncertainty regarding genotypes, which arises from several sources, including mapping and sequencing errors (Korneliussen *et al.*, 2014; Clark *et al.*, 2019).

Statistical analyses

To characterize population structure for all samples without any a-priori partitioning, we first performed a principal component analysis (PCA) of posterior genotype probabilities implemented in PCANGSD (Meisner & Albrechsten, 2018). To test for IBD, we first regressed pairwise kinship coefficients F_{ij} (Loiselle *et al.*, 1995) between individuals and pairwise geographic distances with SPAGEDi v.1.5d (Hardy & Vekemans, 2002). We used both raw and log-transformed distances and selected the best-fit result based upon the r^2 . Significance of the slopes was tested in two ways. First, we performed 1000 random permutations of individuals among sampling points across the entire geographic range (Mantel test). Second, we implemented a Jackknife of the loci to recompute the slope after successively pruning one SNP from the data at a time and estimating the standard deviation of the slope across SNPs, and hence determining whether its 95% confidence interval (i.e. $1.96 \times$ the standard deviation for a significance level of 0.05) encompasses 0, in which case the slope would be considered to be nonsignificant.

To determine whether the IBD signal would be due to strong genetic structures at very short spatial scales, we performed IBD analyses across restricted ranges. In bryophytes, spore densities indeed markedly decrease with increasing distance from the source across the first tens to hundreds of meters (Sundberg, 2005; Lönnell *et al.*, 2012). Spore trapping experiments revealed, however, that the relationship between spore densities and distance becomes nonsignificant after 500 m–1 km, suggesting that, once airborne, spores have no dispersal limitations (Lönnell *et al.*, 2012), which would create the conditions for the applicability of the inverse isolation hypothesis (Szövényi *et al.*, 2012). To test this, we re-ran the analyses, considering only pairs of individuals separated by a distance of > 1 km. Significance of the slope

across restricted distance ranges was assessed by replacing all the distances < 1 km as missing data and assessing the significance of the slope after 1000 permutations of the geographic distance matrix, and a Jackknife across loci.

Second, we used ANGSD to compute pairwise genetic distances between pairs of individuals $d_{ij} = \sum_m^M 1 - I_{b_j}(b_i)$ where $I_{b_j}(b_i)$ is the indicator function, which is equal to 1 when the two individuals i and j have the same base and 0 otherwise, and M is the number of sites with a read for both individuals. A distance of 0 was used as evidence for genotypic identity across loci in the considered species pair, and was used as a proxy for clonality. Given the very low proportion of identical genotypes (Result section), we did not control for clonality in the IBD analyses. We then performed Mantel tests between d_{ij} and pairwise geographic distances.

To compare the results with previous studies on IBD in bryophytes from a meta-analysis of datasets using haplotype frequencies and SNPs (Vanderpoorten *et al.*, 2019), and in particular, to test the hypothesis that differences in the significance of the IBD signal observed come from an increased statistical power associated with the higher number of loci with RADseq data (Discussion), we sub-sampled the data matrix for three species (*A. juliformis*, *B. hookeri* and *S. helicophyllus*). One hundred matrices including 100 randomly sampled SNPs (roughly corresponding to an average of 10 loci with 10 alleles each in Vanderpoorten *et al.*, 2019) were generated, and each matrix was submitted to IBD tests across the entire range and beyond 1000 m.

To compare the fine-scale genetic structure of bryophytes with that of angiosperms, we also computed the S_p statistic, which characterizes the rate of decrease of pairwise kinship coefficients between individuals with the logarithm of the distance (Vekemans & Hardy, 2004). The S_p statistic varies as a function of the mating system and dispersal traits, with low values typically characterizing organisms with high dispersal capacities. The S_p statistic is measured as $-\hat{b}_F / (1 - \hat{F}_1)$, where $-\hat{b}_F$ is the regression slope on the logarithm of distance and \hat{F}_1 is the mean kinship coefficient between individuals belonging to the first distance interval (here, 1 km) that includes all pairs of neighbours. We computed the confidence interval of S_p as $-\hat{b}_F \pm 1.96 \times \text{SE} / (1 - \hat{F}_1)$, where SE is the standard error of the slope, as assessed by Jackknife across loci.

To test for IBE and the impact of geographic barriers, we assigned specimens to one of two groups (terra firme vs white-sand forest and west or east of the Rio Negro) and computed F_{ST} between the two groups. Significance of the observed F_{ST} values was tested by 1000 random permutations of individuals among groups and Jackknife across loci (except for the M3 matrix), as implemented by SPAGEDi.

Data availability

RADseq raw data were submitted to the NCBI Sequence Read Archive (SRA) with bioproject accession no. PRJNA530510. Sequence data are available from GenBank (bioproject PRJNA530510).

Table 1 Average number of raw reads, number of allele clusters, percentage of allele clusters filtered out to ensure a minimum of 3 reads per allele (% read depth, %RD), percentage of heterozygous allele clusters filtered out (%He) and number of loci (mean loci), among individuals, along with total number of loci (tot loci) together with number of SNPs (N), average percentage of sequenced SNPs per individual (%SNPs) and number of individuals (n) in data matrices M1 and M2 for 10 Amazonian bryophytes species, as well as mean and standard deviation (SD) of the same variables among all species.

	Raw reads	Allele clusters	%RD	%He	Mean loci	Tot loci	N(M2)	N(M1)	% SNPs (M2)	% SNPs (M1)	nM2	nM1
<i>Archilejeunea juliformis</i> (Nees) Gradst.	1474 403	794 027	78	16	7814	33 963	362	33 284	38	18	38	23
<i>Bazzania hookeri</i> (Lindenb.) Tre-vis.	2188 823	1182 346	79	14	5278	14 729	860	14 648	34	29	23	14
<i>Leucobryum martianum</i> (Hornsch.) Hampe ex Müll. Hal.	1767 423	992 325	80	14	10 909	64 079	143	12 162	40	22	41	29
<i>Micropterigium trachyphyllum</i> Reimers	1677 308	945 706	79	16	3157	6915	2107	6820	42	36	13	12
<i>Octoblepharum albidum</i> Hedw.	1647 361	917 278	81	15	4910	18 030	268	17 666	40	26	26	15
<i>Octoblepharum pulvinatum</i> (Dozy & Molk.) Mitt.	1783 417	964 060	81	15	10 111	42 812	453	41 866	40	22	31	18
<i>Syrrophodon annotinus</i> W.D. Reese & D.G. Griffin	1538 315	770 311	76	14	5825	11 143	183	10 339	37	21	40	25
<i>Syrrophodon helicophyllus</i> Mitt.	2076 985	1136 967	82	14	6811	22 266	984	22 168	34	19	27	24
<i>Syrrophodon hornschuchii</i> Mart.	1691 457	960 142	80	15	4605	13 025	892	12 954	36	24	22	18
<i>Thysananthus amazonicus</i> (Spruce) Steph.	1756 805	1040 260	81	15	2537	4839	1660	4828	39	30	15	15
Mean \pm SD	1760 230 \pm 221 087	970 343 \pm 130 276	80 \pm 2	15 \pm 1	6196 \pm 2755	23 180 \pm 18 625	782 \pm 666	17 674 \pm 11 774	38 \pm 3	25 \pm 6	28 \pm 10	19 \pm 6

Results

RADseq raw data were submitted to the NCBI Sequence Read Archive with reference number PRJNA530510. Accession numbers for each individual can be found in Table S1. An average total of 17.6 million reads ($\pm 13\%$) per individual was obtained across species (Table 1). From those reads, the clustering of alleles diverging by a maximum of 15% within individuals led to an average of 9.7 million allele clusters ($\pm 13\%$) per individual. The read depth filtering led to the loss of an average of $80 \pm 2\%$ of the allele clusters. The filtering-out of heterozygous allele clusters led to the loss of another $15 \pm 1\%$ of them. The clustering of allele clusters diverging by a maximum of 15% among individuals led to an average of 6196 ± 2726 loci genotyped per individual across species. After the random selection of a single SNP per locus, we ended up with matrices including an average of 17 674 (min 4828, max 41 866) and 782 (min 143, max 2107) SNPs for M20 and M35, respectively. In these matrices, $26 \pm 6\%$ (min 20, max 36) and $38 \pm 3\%$ (min 35, max 42) of the SNPs were sequenced on average per specimen per species for M1 and M2, respectively (Table 1).

The PCAs of posterior genotype probabilities revealed no spatial structure in the data (Fig. S1). Furthermore, genotypic identity was found only in three species in very low proportions (*B. hookeri*, 2 out of 253 pairs; *O. albidum*, 4 out of 300 pairs; and *S. annotinus*, 2 out of 741 pairs).

The slope of the regression analyses between kinship coefficients and geographic distance and their P -value, the F_{ST} between populations from terra firme and white-sand forest on the one hand, and between populations separated by the Rio Negro on the other, and their P -values, and the 'Sp' statistics are presented in Table 2. The slope of the regressions between the genetic distances between pairs of individuals generated by ANGSD and geographic distance across the entire geographic range was significant for 8 out of the 10 investigated species, and remained significant for pairs of individuals located at > 1 km from each other. Similar results were obtained with the analysis of the SNP matrix, but significant IBD patterns were recovered by either the M1 or M2 matrix, but not both, in most cases. The spatial autocorrelograms resulting from the regression between kinship coefficients and geographic distance are shown in Fig. 2. The Sp statistic was 0.012 on average across species, with a minimum of 0.006 in *S. helicophyllus* and a maximum of 0.038 in *S. annotinus*.

The power of the IBD tests for pairs of individuals located at > 1 km from each other was significantly lower in the analyses of the 100 reduced data matrices including 100 randomly selected SNPs than in the full SNP data matrices. In fact, the standard deviation of the IBD slope computed among pairs of individuals located at > 1 km from each other, $b_{>1}$, was systematically lower than the range of the standard deviations obtained for $b_{>1}$ across 100 reduced data matrices including 100 randomly selected SNPs. Thus in *A. juliformis*, the standard deviation of $b_{>1}$ for the complete SNP matrix was 0.008 but had an average of 0.017 ± 0.003 across the 100 matrices of 100 randomly selected SNPs. In *B. hookeri* and *S. helicophyllus*, these values were 0.011 vs

0.037 ± 0.010 and 0.008 vs 0.024 ± 0.005 , respectively (Table S2). Therefore, among the 100 randomly sub-sampled matrices of 100 SNPs, 61 significant IBD patterns across the entire geographic range, 32 of which remained significant at > 1 km, were recovered in *A. juliformis*. In *B. hookeri* and *S. helicophyllus*, these numbers were 40 and 16, and 26 and 4, respectively (Table S2).

Evidence for differentiation due to soil type or geographic barriers was very weak. Significant F_{ST} between populations separated by the Rio Negro were found in four species, but the results were very inconsistent across analyses. For example, both randomization and Jackknife tests returned significant F_{ST} with the M2 matrix in *L. martianum* and *S. annotinus*, but this result was not confirmed by the analyses performed with ANGSD (M3 matrix). In terra firme vs white-sand forest comparisons, the permutation test returned a significant F_{ST} value in *A. juliformis* with the M1 matrix, but this was not supported by the Jackknife test for the same matrix nor by analyses with the two other matrices (Table 2).

Discussion

In sharp contrast to our initial hypothesis that Amazonian bryophytes exhibit high dispersal capacities eroding any signal of IBD at the landscape scale, significant spatial population structure was observed in 8 out of 10 investigated species and remained significant beyond the range of short-distance dispersal, thus offering evidence contrary to the inverse isolation hypothesis. Mounting evidence for significant genetic structures contrasts with the widely accepted notion that bryophytes disperse freely across the landscape (Medina *et al.*, 2011) and challenges, in particular, the idea that Amazonian bryophyte species 'behave as one single metacommunity' based on their homogeneous distributions at very large spatial scales. (Mota de Oliveira & ter Steege, 2015).

As a comparison, the average Sp statistic across species lies in the range reported for angiosperm species characterized by wind dispersal (Vekemans & Hardy, 2004). Although the high Sp values reported here may partly result from the low density of the sampled populations (Vekemans & Hardy, 2004), it is especially striking to consider that, within the same Amazonian environment, the average Sp in bryophytes is comparable to that of the Brazil nut tree *Bertholletia excelsa* ($Sp = 0.01\text{--}0.03$) (Sujii *et al.*, 2015) and to that of natural populations of the palm tree *Astrocaryum aculeatum* ($Sp = 0.014$) (Ramos *et al.*, 2016), whereas bryophytes diaspores are much smaller ($c. 20 \mu\text{m}$) than those of the latter ($c. 30 \text{ mm}$ in *A. aculeatum* and enclosure of seeds within a 10–16 cm globose, functionally indehiscent woody capsule in *B. excelsa*). The strong IBD pattern revealed here is, nonetheless, consistent with the dispersal traits of the studied species, including the absence of male expression (*S. annotinus*, Pereira *et al.*, 2016), the prevalence of dioicy in Calymperaceae associated with low sporophyte production (Pereira *et al.*, 2019b), the immersion of the sporophytes within perichaetial leaves or very short setae (*S. annotinus*, *S. helicophyllus*), and reduced peristomes (*S. annotinus*, *S. hornschi*). This strong IBD pattern is also consistent with

Table 2 Summary statistics of the genetic structure of Amazonian bryophytes. $b(p)$ and $b(1)(p)$ are the slopes of the regression between F_{ij} and geographic distance (either linear distances b -lin or their log-transformation b -log, depending on the r^2 of the regression) across the entire range and for pairs of individuals located at > 1 km from each other, respectively.

	$b \pm SE$	r^2	$b(1) \pm SE$	r^2	$F_{ST-GB} \pm SD$	$F_{ST-IBE} \pm SD$	Sp
<i>Archilejeunea juliformis</i> ($n = 38$)							
					$n_E = 26,$ $n_W = 12$	$n_{TF} = 14,$ $n_{WFSF} = 24$	
M1	b -lin = $-5.08 \pm 2.28 \times 10^{-5}$	9×10^{-4}	b -log = $-0.0062^* \pm 0.0015$	0.003	0.00 ± 0.50	$0.14^{**} \pm 0.51$	–
M2	b -lin = – $5.78^{***} \pm 1.50 \times 10^{-4}$	0.02	b -lin = – $4.47^{***} \pm 1.50 \times 10^{-4}$	0.02	0.03 ± 0.019	0.01 ± 0.017	(0.008) 0.021 (0.032)
M3	b -lin = 0.0036^{***}	0.19	b -lin = $4.70 \times 10^{-5}^{***}$	0.20	0.06	0.03	–
<i>Bazzania hookeri</i> ($n = 23$)							
					$n_E = 16,$ $n_W = 7$	$n_{TF} = 2,$ $n_{WFF} = 21$	
M1	b -lin = -6.48×10^{-6} $\pm 4.48 \times 10^{-5}$	0.12	b -log = 0.007 ± 0.0041	0.002	0.00 ± 0.46	NA	–
M2	b -lin = – $5.19^{***} \pm 1.50 \times 10^{-4}$	0.05	b -lin = – $5.28^{***} \pm 1.50 \times 10^{-4}$	0.04	0.00 ± 0.010	NA	(0.004) 0.019 (0.033)
M3	b -lin = 0.0019^{***}	0.06	b -lin = $3.24 \times 10^{-5}^{***}$	0.07	0.07	NA	–
<i>Leucobryum martianum</i> ($n = 41$)							
					$n_E = 23,$ $n_W = 18$	$n_{TF} = 9,$ $n_{WFF} = 32$	
M1	b -log = $-0.0150^{**} \pm 0.0018$	0.02	b -log = $-0.0120^{**} \pm 0.0027$	0.007	0.02 ± 0.35	0.01 ± 0.51	(0.011) 0.016 (0.018)
M2	b -log = -0.0111 ± 0.012	< 0.01	b -log = -0.0084 ± 0.0198	< 0.01	$0.06^{**} \pm 0.02$	0.00 ± 0.025	–
M3	b -lin = $2.53 \times 10^{-5}^{***}$	0.05	b -lin = $2.73 \times 10^{-5}^{***}$	0.06	0.02	0.03	–
<i>Micropterygium trachyphyllum</i> ($n = 13$)							
					$n_E = 5, n_W = 8$	$n_{TF} = 4,$ $n_{WFF} = 9$	
M1	b -lin = -4.84×10^{-4} $^{**} \pm 4.38 \times 10^{-5}$	0.23	b -log = $-0.037^{**} \pm 0.003$	0.25	0.01 ± 0.50	0.00 ± 0.46	(0.021) 0.026 (0.028)
M2	b -lin = $-3.39 \times 10^{-4}^{**} \pm 0.002$	0.11	b -log = $-0.027^{**} \pm 0.005$	0.15	0.01 ± 0.59	0.00 ± 0.020	(0.007) 0.015 (0.023)
M3	b -lin = $2.32 \times 10^{-5}^{***}$	0.13	b -lin = $2.49 \times 10^{-5}^{***}$	0.14	0.09	0.02	–
<i>Octoblepharum albidum</i> ($n = 26$)							
					$n_E = 14,$ $n_W = 12$	$n_{TF} = 14,$ $n_{WFF} = 12$	
M1	b -lin = $-1.69 \pm 1.60 \times 10^{-4}$	0.005	b -log = $-1.74 \pm 1.64 \times 10^{-4}$	0.006	0.00 ± 0.50	0.00 ± 0.49	–
M2	b -log = $-0.0240^{**} \pm 0.010$	0.007	b -log = -0.016 ± 0.012	0.004	0.000 ± 0.024	0.00 ± 0.016	(0.005) 0.0188 (0.042)
M3	b -lin = $2.72 \times 10^{-5}^{***}$	0.04	b -lin = $2.62 \times 10^{-5}^{***}$	0.04	0.04^*	0.02	–
<i>Octoblepharum pulvinatum</i> ($n = 31$)							
					$n_E = 10,$ $n_W = 21$	$n_{TF} = 8,$ $n_{WFF} = 23$	
M1	b -lin = $-2.02 \pm 2.13 \times 10^{-4}$	0.013	b -lin = $-2.02 \pm 2.16 \times 10^{-4}$	0.014	0.01 ± 0.69	0.00 ± 0.74	–
M2	b -lin = 6.29×10^{-5} $\pm 8.25 \times 10^{-5}$	0.0006	b -log = 0.0108 ± 0.007	0.003	0.00 ± 0.01	0.02 ± 0.018	–
M3	b -lin = 1.27×10^{-6}	0.0002	b -lin = 3.55×10^{-6}	0.002	0.03	0.04	–
<i>Syrhobodon annotinus</i> ($n = 40$)							
					$n_E = 23,$ $n_W = 17$	$n_{TF} = 0,$ $n_{WFF} = 40$	
M1	b -lin = $-3.75^{**} \pm 1.54 \times 10^{-4}$	0.008	b -lin = – $3.68^{**} \pm 1.57 \times 10^{-4}$	0.007	0.03 ± 0.007	NA	(0.009) 0.011 (0.030)
M2	b -log = $-0.0337^{***} \pm 0.009$	0.02	b -log = $-0.0432^{***} \pm 0.0164$	0.015	$0.06^{**} \pm 0.024$	NA	(0.014) 0.038 (0.051)
M3	b -lin = 2.29×10^{-5} (0.002)	0.02	b -lin = 2.44×10^{-5} (< 0.001)	0.02	0.02	NA	–
<i>Syrhobodon helicophyllum</i> ($n = 27$)							
					$n_E = 23,$ $n_W = 4$	$n_{TF} = 0,$ $n_{WFF} = 27$	
M1	b -lin = -0.0003 ± 0.0014		b -lin = 0.0056 ± 0.0026		0.03 ± 0.007	NA	–
M2	b -log = $-0.014^{\dagger} \pm 0.011$	0.004	b -log = -0.022 ± 0.021	0.003	0.10 ± 0.08	NA	(0.007) 0.014 (0.035)
M3	b -lin = $2.59 \times 10^{-5}^{***}$	0.05	b -lin = $2.35 \times 10^{-5}^{***}$	0.03	0.05	NA	–
<i>Syrhobodon hornsuschii</i> ($n = 22$)							
					$n_E = 14,$ $n_W = 8$	$n_{TF} = 17,$ $n_{WFF} = 5$	
M1	b -log = $-0.0089^* \pm 0.0016$	0.031	b -lin = -1.77×10^{-4} $^* \pm 3.69 \times 10^{-5}$	0.02	0.00 ± 0.67	0.00 ± 0.66	(0.005) 0.0093 (0.012)
M2	b -lin = $-4.33 \pm 7.28 \times 10^{-5}$	7×10^{-4}	b -lin = $-6.60 \pm 7.60 \times 10^{-5}$	0.002	0.00 ± 0.016	0.003 ± 0.015	–
M3	b -lin = $3.30 \times 10^{-5}^{***}$	0.16	b -lin = $3.22 \times 10^{-5}^{***}$	0.14	0.03	0.04	–

Table 2 (Continued)

	$b \pm SE$	r^2	$b(1) \pm SE$	r^2	$F_{ST-GB} \pm SD$	$F_{ST-IBE} \pm SD$	Sp
<i>Thysananthus amazonicus</i> ($n = 15$)					$n_E = 12,$ $n_{VV} = 3$	$n_{TF} = 0,$ $n_{WFF} = 15$	
M1	$b\text{-lin} = -2.70 \times 10^{-5}$ $\pm 1.28 \times 10^{-4}$	0.0001	$b\text{-lin} = -5.88 \times 10^{-5}$ $\pm 1.66 \times 10^{-4}$	0.0005	0.00 ± 0.67	NA	–
M2	$b\text{-lin} = 8.24 \pm 4.52 \times 10^{-5}$	0.009	$b\text{-lin} = -2.37 \pm 5.71 \times 10^{-4}$	0.04	0.00 ± 0.020	NA	–
M3	$b\text{-lin} = -2.95 \times 10^{-6}$	0.009	$b\text{-lin} = -9.32 \times 10^{-6}$	0.04	0.04	NA	–

SE is the standard error of the slope, as assessed by Jackknife across loci (except for the M3 matrices, which are not based on SNP calls). Slopes whose confidence intervals (i.e. $b \pm 1.96 SE$) do not encompass 0 are considered to be significant. F_{ST-GB} and F_{ST-IBE} are the F_{ST} between populations separated by the Rio Negro and occurring on different forest types (terra firme vs white-sand forest), respectively. Sp is the Sp statistic, a measure of the rate of decrease of pairwise kinship coefficients between individuals with the logarithm of the distance (Vekemans & Hardy, 2004). The lower and upper bounds of the confidence interval of Sp are given in parentheses. Sp statistics were not computed when the IBD slope was not significant, which is indicated by a minus symbol (–) in the relevant column. M1, M2 and M3 are the data matrices produced by IPYRAD with different levels of missing data (M1–M2) and by ANGSD (M3). Significant statistics (*, $P < 0.05$; **, $P < 0.01$; ***, $P < 0.001$) are in bold. NA indicates that the statistics could not be computed (species restricted to a single forest type).

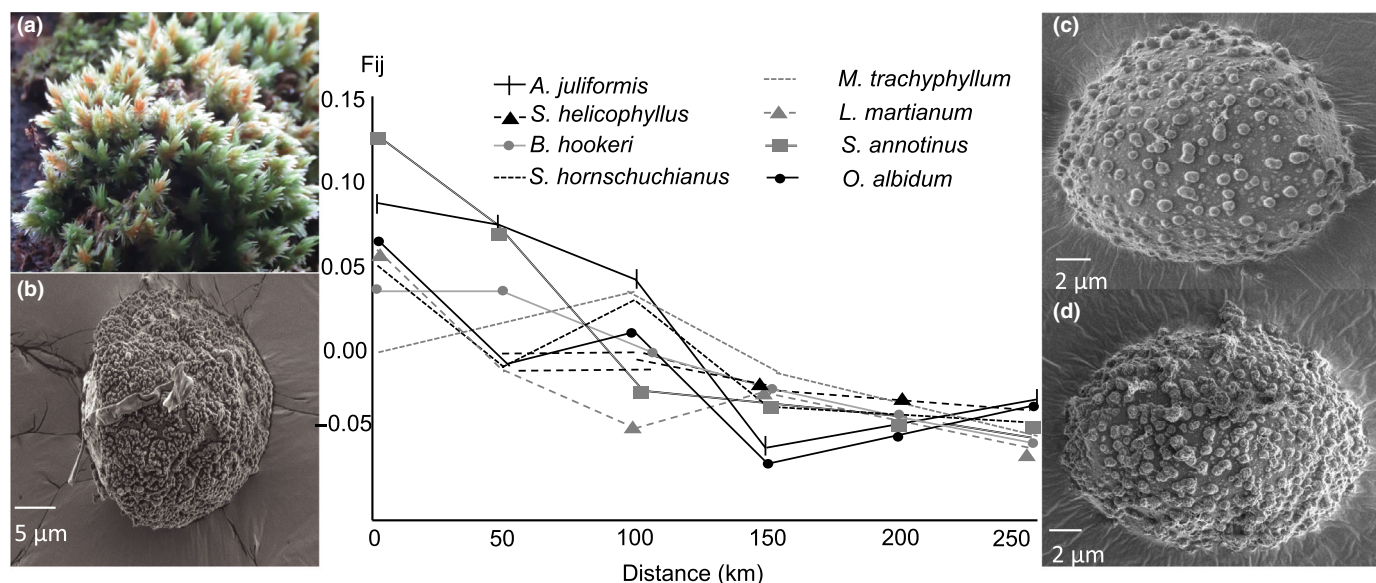


Fig. 2 Spatial autocorrelation of the variation of kinship coefficients F_{ij} derived from SNP variation between pairs of individuals as a function of geographic distance in eight bryophyte species showing significant isolation-by-distance slopes (see Table 2 for slope and P -values) in central Amazonia. (a) *Leucobryum martianum*, habit. (b–d) SEM photographs of spores (distal view) of *L. martianum*, *Octoblepharum albidum* and *Octoblepharum pulvinatum*, respectively.

the fact that, while bryophyte species are mostly wind-dispersed (see Patiño & Vanderpoorten, 2018 for review), anemochorous plants in dense tropical rainforests typically exhibit tighter clusters than animal-dispersed species because of the barriers imposed by the dense forest canopy on wind speed (Seidler & Plotkin, 2006). In such conditions, zoochory, whose significance has been increasingly evidenced in bryophytes (Chmielewski & Eppley, 2019; Russo *et al.*, 2020, and references therein), including by bats in tropical forest environments (Parsons *et al.*, 2007), might play an important role.

Significant IBD patterns are thus reported here despite the comparatively lower number of SNPs than in recent population genetic studies based on RADseq in bryophytes (Baughman *et al.*, 2017; Lewis *et al.*, 2017) and angiosperms, wherein 2000–3000 independent SNPs are commonly reported for

phylogeographic studies (e.g. Prunier *et al.*, 2017; Bell *et al.*, 2018). In the present study, a substantial drop in the number of allele clusters occurred when applying the recommended minimum number of raw reads required to form an allele (Paris *et al.*, 2017). This may have been caused by the use of a restriction enzyme with a high frequency of target sites, resulting in a multitude of DNA fragments in relation to the low number of reads per fragment (low read depth), thus calling for the use of two restriction enzymes (ddRAD) in future studies. More consistent IBD patterns were recovered by analyses based on genotype likelihoods than by analyses based on SNP calling, whose significance varied, but not systematically in the same direction, depending on the level of missing data. Our results therefore support the idea that analyses based on genotype likelihoods perform better than analyses based on genotype calls with NGS data

characterized by low read depth and high levels of missing data (Korneliusson *et al.*, 2014; Meisner & Albrechsten, 2018; Klonoski *et al.*, 2019).

Most importantly, however, the strong population genetic structure reported herein at the landscape scale unambiguously shows that these data are suitable for testing the proposed hypotheses. In particular, a persisting signal of IBD was consistently reported beyond the range of short-distance dispersal (> 1 km). This contrasts with a recent meta-analysis of fine-scale spatial genetic structures in bryophytes, which reported the decay of the IBD pattern beyond that range in 30–50% of the datasets investigated (Vanderpoorten *et al.*, 2019). We interpret the differences between the present and previous studies on IBD in bryophytes in terms of statistical power of the tests, since previous studies were based on haplotypic or SNP variation at a few loci. This interpretation is supported by our sub-sampling analysis of three datasets, which revealed that, for a similar number of polymorphic markers as in Vanderpoorten *et al.* (2019), we observed significantly higher standard deviations of the IBD slopes between pairs of individuals located at > 1 km from each other in the randomly subsampled data matrices than in the full matrices, with a corresponding decay of the significance of the IBD signal beyond 1 km.

Given the strong spatial limitations reported here, one potential issue could be that the geographical scale of our sampling was too large to correctly infer IBD, as other historical factors than IBD *per se* could potentially contribute to the observed geographic structures. The very homogeneous climate conditions that prevail across hundreds of kilometres of the flat Amazonian landscape, the absence of any apparent ecological or geographic grouping of individuals in the PCA, and the failure of F_{ST} analyses to consistently highlight spatial structures associated with differences among main forest types and geographic position with regard to the potential geographic barrier of the Rio Negro, do not support such a hypothesis. In fact, and although the very large confidence intervals of the F_{ST} suggest that additional population and molecular sampling could potentially reveal a stronger ecological structure in the data than revealed by the present analyses, our results are not consistent with the idea that IBE and the presence of geographic barriers have shaped the genetic structure of bryophyte species. This is in line with our predictions and in contrast to Wallace's hypothesis (Ortiz *et al.*, 2018) and the gradient hypothesis (Guevara *et al.*, 2016), both of which postulate a strong imprint of the Amazonian hydrographic network and variation in soil conditions, respectively, on the genetic structure of Amazonian biota. While in angiosperms a signature of IBE was found in a meta-analysis in about 20% of the cases (Sexton *et al.*, 2014), and while, within Amazonia specifically, evidence for ecotypic differentiation between white-sand forest and terra firme populations is suggestive of an adaptive mechanism of edaphic specialization (Fine *et al.*, 2013; Fine & Baraloto, 2016), the absence of significant differences of allele frequencies between terra firme and white-sand forest populations in the investigated bryophytes is in line with the idea that bryophytes exhibit 'multi-purpose' genotypes and fail to diversify in response to environmental heterogeneity (Patiño *et al.*, 2014).

In turn, the absence of significant differences in allele frequencies between populations separated by the Rio Negro is, at first sight, at odds with the fairly severe dispersal limitations revealed by the IBD analyses. We suggest that the Rio Negro is not a barrier for wind-dispersed organisms like bryophytes because, instead of being a continuous stretch of water, it is a mosaic of streams and sand islands potentially acting as stepping stones. Connectivity may especially have been strong during the glacial periods of the Pleistocene, when the global Amazonian climate was much drier than today (Cheng *et al.*, 2013). In these conditions, spores may have the dispersal capacity to overcome the natural fragmentation of the landscape by the hydrographic network, in line with growing evidence in flying or wind-dispersed organisms such as birds, butterflies and vascular plants (Dambros *et al.*, 2017; Santorelli *et al.*, 2018).

Altogether, our results thus suggest that Amazonian bryophytes exhibit substantial spatial genetic structure that points to unexpected dispersal limitation in light of the reproductive strategies and life-history characteristics of cryptogams in general. This raises substantial concerns about the immigration/extinction balance in such populations of cryptogamic biodiversity in the botanically richest biome on the planet, which remains under imminent threat from anthropogenic disturbances.

Acknowledgements

Many thanks are due to Norm Wickett for introducing AL to genomics during a research stay at Chicago Botanic Garden and to three referees for their comments on the manuscript. Financial support from a bilateral agreement of scientific cooperation between the Belgian and Brazilian Science Foundations (FRS-FNRS and CNPq, grant 56526) is gratefully acknowledged. AV and AL are, respectively, research director and PhD student funded by the Belgian Science Foundation.

Author contributions


AV designed the study. AL, MP, CEZ, SRG and AV sampled, analyzed and prepared the specimens. MdH, PB and IVdB produced SEM pictures of spores. AL and RO produced the data. AL, JG, BL, PM and AV analyzed the data. AV and CEZ wrote the manuscript with the assistance of all co-authors. AL and JG contributed equally to this work.

ORCID

Jérémy Gauthier  <https://orcid.org/0000-0001-6666-1002>

S. Robbert Gradstein  <https://orcid.org/0000-0002-3849-6457>

Alice Ledent  <https://orcid.org/0000-0003-3024-8720>

Patrick Mardulyn  <https://orcid.org/0000-0003-2154-5256>

Alain Vanderpoorten  <https://orcid.org/0000-0002-5918-7709>

Charles E. Zartman  <https://orcid.org/0000-0001-8481-9782>

References

- Adeney JM, Christensen N, Vincenti A, Cohn Haft M. 2016. White-sand ecosystems in Amazonia. *Biotropica* 48: 7–23.
- Barb  M, Fenton NJ, Bergeron Y. 2016. So close and yet so far away: long-distance dispersal events govern bryophyte metacommunity reassembly. *Journal of Ecology* 104: 1707–1719.
- Baughman JT, Payton AC, Paasch AE, Fisher KM, McDaniel SF. 2017. Multiple factors influence population sex ratios in the Mojave Desert moss *Syntrichia caninervis*. *American Journal of Botany* 104: 733–742.
- Bell N, Griffin PC, Hoffmann AA, Miller AD. 2018. Spatial patterns of genetic diversity among Australian alpine flora communities revealed by comparative phylogenomics. *Journal of Biogeography* 45: 177–189.
- Benavides JC, Duque AJ, Duivenvoorden JF, Cleef AM. 2016. Species richness and distribution of understory bryophytes in different forest types in Colombian Amazonia. *Journal of Bryology* 28: 182–189.
- Campos Salazar LV. 2016. *Diversity of epiphytic bryophytes of the Amazon*. Bogot , Colombia: Dissertation, Universidad Nacional de Colombia.
- Cheng H, Sinha A, Cruz FW, Wang X, Edwards RL, d'Horta FM, Ribas CC, Vuille M, Stott LD, Auler AS. 2013. Climate change patterns in Amazonia and biodiversity. *Nature Communications* 4: 1411.
- Chmielewski MW, Eppley SM. 2019. Forest passerines as a novel dispersal vector of viable bryophyte propagules. *Proceedings of the Royal Society B* 286: 20182253.
- Clark LV, Lipka AE, Sacks EJ. 2019. polyRAD: Genotype calling with uncertainty from sequencing data in polyploids and diploids. *G3: Genes, Genomes, Genetics* 9: 663–673.
- Cornelissen JHC, Ter Steege H. 1989. Distribution and ecology of epiphytic bryophytes and lichens in dry evergreen forests of Guyana. *Journal of Tropical Ecology* 5: 131–150.
- Costa FM, Terra-Araujo MH, Zartman CE, Cornelius C, Carvahlo FA, Hopkins MJG, Viana PL, Prata EMB, Vicentini A. 2019. Islands in a green ocean: Spatially structured endemism in Amazonian white-sand vegetation. *Biotropica* 52: 34–45.
- Dambros CS, Morais JW, Azevedo RA, Gotelli NJ. 2017. Isolation by distance, not rivers, control the distribution of termite species in the Amazonian rain forest. *Ecography* 40: 1242–1250.
- Elshire RJ, Glaubitz JC, Sun Q, Poland JA, Kawamoto K, Buckler ES, Mitchell SE. 2011. A robust, simple genotyping-by-sequencing (GBS) approach for high diversity species. *PLoS ONE* 6: e19379.
- Fine PVA, Baraloto C. 2016. Habitat endemism in white-sand forests: insights into the mechanisms of lineage diversification and community assembly of the Neotropical flora. *Biotropica* 48: 24–33.
- Fine PVA, Zapata F, Daly DC, Mesones I, Misiewicz TM, Cooper HF, Barbosa CEA. 2013. The importance of environmental heterogeneity and spatial distance in generating phylogenetic structure in edaphic specialist and generalist tree species of *Protium* (Burseraceae) across the Amazon Basin. *Journal of Biogeography* 40: 646–661.
- Guevara JE, Damasco G, Baraloto C, Fine PVA, Pe uela MC, Castilho C, Vicentini A, C rdenas D, Wittmann F, Targhetta N *et al.* 2016. Low phylogenetic beta diversity and geographic neo-endemism in Amazonian white-sand forests. *Biotropica* 48: 34–46.
- Hardy OJ, Vekemans X. 2002. SPAGeDi: a versatile computer program to analyze spatial genetic structure at the individual or population levels. *Molecular Ecology Notes* 2: 618–620.
- Hodel RGJ, Chen S, Payton AC, McDaniel SF, Soltis P, Soltis DE. 2017. Adding loci improves phylogeographic resolution in red mangroves despite increased missing data: comparing microsatellites and RAD-Seq and investigating loci filtering. *Scientific Reports* 7: 17598.
- Hol  E, Ko nar J, Ku era J. 2015. Comparison of genetic structure of epixylic liverwort *Crossocalyx hellerianus* between central European and fennoscandian populations. *PLoS ONE* 10: e0133134.
- Hoorn C, Wesselingh FP. 2010. *Amazonia: landscape and species evolution. A look into the past*. Oxford, UK: Wiley & Sons.
- Hutsem kers V, Hardy O, Mardulyn P, Shaw AJ, Vanderpoorten A. 2010. Macroecological patterns of genetic structure and diversity in the aquatic moss *Platyhypnidium riparioides*. *New Phytologist* 185: 852–864.
- Hutsem kers V, Hardy OJ, Vanderpoorten A. 2013. Does water facilitate gene flow in spore-producing plants? Insights from the fine-scale genetic structure of the aquatic moss *Rhynchostegium riparioides* (Brachytheciaceae). *Aquatic Botany* 108: 1–6.
- Klonoski K, Bi K, Rosenblum EB. 2019. Phenotypic and genetic diversity in aposematic Malagasy poison frogs (genus *Mantella*). *Ecology and Evolution* 9: 2725–2742.
- Korneliussen TS, Albrechtsen A, Nielsen R. 2014. ANGSD: analysis of next generation sequencing data. *BMC Bioinformatics* 15: 356.
- Korpelainen H, von Cr utlein M, Kostamo K, Virtanen V. 2013. Spatial genetic structure of aquatic bryophytes in a connected lake system. *Plant Biology* 15: 514–521.
- Korpelainen H, von Cr utlein M, Laaka-Lindberg S, Huttunen S. 2011. Fine-scale spatial genetic structure of a liverwort (*Barbilophozia attenuata*) within a network of ant trails. *Evolutionary Ecology* 25: 45–57.
- Korpelainen H, Forsman H, Virtanen V, Pietil inen M, Kostamo K. 2012. Genetic composition of bryophyte populations occupying habitats differing in the level of human disturbance. *International Journal of Plant Sciences* 173: 1015–1022.
- Lewis LR, Biersma EM, Carey SB, Holsinger K, McDaniel SF, Rozzi R, Goffinet B. 2017. Resolving the northern hemisphere source region for the long-distance dispersal event that gave rise to the South American endemic dung moss *Tetraplodon fuegianus*. *American Journal of Botany* 104: 1651–1659.
- Li H, Durbin R. 2009. Fast and accurate short read alignment with Burrows-Wheeler transform. *Bioinformatics* 25: 1754–1760.
- Loiselle BA, Sork VL, Nason J, Graham C. 1995. Spatial genetic structure of a tropical understory shrub, *Psychotria officinalis* (Rubiaceae). *American Journal of Botany* 82: 1420–1425.
- L nnell N, Hylander K, Jonsson BG, Sundberg S. 2012. The fate of the missing spores – patterns of realized dispersal beyond the closest vicinity of a sporulating moss. *PLoS ONE* 7: e41987.
- Mar  MLG, Toledo JJ, Nascimento HEM, Zartman CE. 2016. Regional and fine scale variation of holoeiphyte community structure in Central Amazonian white-sand forests. *Biotropica* 48: 70–80.
- Medina NG, Draper I, Lara F. 2011. Biogeography of mosses and allies: does size matter? In: Fontaneto D, ed. *Biogeography of micro-organisms. Is everything small everywhere?* Cambridge, UK: Cambridge University Press, 209–233.
- Meisner J, Albrechtsen A. 2018. Inferring population structure and admixture proportions in low depth NGS data. *Genetics* 210: 719–731.
- Mikulaskova E, Hajek M, Veleba A, Johnson MG, Hajek T, Shaw AJ. 2014. Local adaptations in bryophytes revisited: the genetic structure of the calcium-tolerant peatmoss *Sphagnum warnstorffii* along geographic and pH gradients. *Ecology and Evolution* 5: 229–242.
- Mota de Oliveira S, Temme A, Erken R, ter Steege H. 2011. Dispersal and connectivity of populations of *Cheilelejeunea rigidula* (Lejeuneaceae) in Amazonian forests: a pilot study. *Boletim do Instituto de Bot nica* 21: 133–139.
- Mota de Oliveira S, ter Steege H. 2015. Bryophyte communities in the Amazon forest are regulated by height on the host tree and site elevation. *Journal of Ecology* 102: 441–450.
- Nazareno AG, Dick CW, Lohmann LG. 2019. A biogeographic barrier test reveals a strong genetic structure for a canopy-emergent Amazon tree species. *Scientific Reports* 9: 18602.
- Ortiz DA, Lima AP, Werneck F. 2018. Environmental transition zone and rivers shape intraspecific population structure and genetic diversity of an Amazonian rain forest tree frog. *Evolutionary Ecology* 32: 359–378.
- Paris JR, Stevens JR, Catchen JM. 2017. Lost in parameter space: a road map for STACKS. *Methods in Ecology and Evolution* 8: 1360–1373.
- Parsons JG, Cairns A, Johnson CN, Robson SKA, Shilton LA, Westcott DA. 2007. Bryophyte dispersal by flying foxes: a novel discovery. *Oecologia* 152: 112–114.
- Pati o J, Carine MA, Fern ndez-Palacios JM, Otto R, Schaefer H, Vanderpoorten A. 2014. The anagenetic world of spore-producing land plants. *New Phytologist* 201: 305–311.
- Pati o J, Vanderpoorten A. 2018. Bryophyte biogeography. *Critical Reviews in Plant Sciences* 37: 175–209.
- Pereira MR, C mara PEAS, Amorim BS, McDaniel SF, Payton AC, Carey SB, Sierra AM, Zartman CE. 2019b. Advances in Calymperaceae (Dicranidae,

- Bryophyta): phylogeny, divergence times and pantropical promiscuity. *The Bryologist* 122: 183–196.
- Pereira MR, Dambros CS, Zartman CE. 2016. Prezygotic resource-allocation dynamics and reproductive trade-offs in Calymperaceae (Bryophyta). *American Journal of Botany* 103: 1–9.
- Pereira MR, Ledent A, Mardulyn P, Zartman CE, Vanderpoorten A. 2019a. Maintenance of genetic and morphological identity in two sibling *Syrrophodon* species (Calymperaceae, Bryopsida) despite extensive introgression. *Journal of Systematics and Evolution* 57: 395–403.
- Punier R, Akman M, Kremer CT, Aitken N, Chuah A, Borevitz J, Holsinger KE. 2017. Isolation by distance and isolation by environment contribute to population differentiation in *Protea repens* (Proteaceae L.), a widespread South African species. *American Journal of Botany* 104: 674–684.
- Ramos SLF, Dequigiovanni G, Sebbenn AM, Gomes Lopes MT, Kageyama PY, Vasconcelos de Macêdo JL, Kirst M, Veasey EA. 2016. Spatial genetic structure, genetic diversity and pollen dispersal in a harvested population of *Astrocaryum aculeatum* in the Brazilian Amazon. *BMC Genetics* 17: 63.
- Russo NJ, Robertson M, MacKenzie R, Goffinet B, Jiménez JE. 2020. Evidence of targeted consumption of mosses by birds in sub-Antarctic South America. *Austral Ecology* 45: 399–403.
- Santorelli S, Magnusson WE, Deus CP. 2018. Most species are not limited by an Amazonian river postulated to be a border between endemism areas. *Scientific Reports* 8: 2294.
- Schuster RM. 1983. Phytogeography of the bryophyta. In: Schuster RM, ed. *New manual of bryology, vol. 1*. Nichinan, Japan: The Hattori Botanical Laboratory, 463–626.
- Seidler TG, Plotkin JB. 2006. Seed dispersal and spatial pattern in tropical trees. *PLoS Biology* 4: e344.
- Sexton JP, Hangartner SB, Hoffmann AA. 2014. Genetic isolation by environment or distance: which pattern of gene flow is most common? *Evolution* 68: 1–15.
- Shaw AJ. 1992. The evolutionary capacity of bryophytes and lichens. In: Bates JW, Farmer AM, eds. *Bryophytes and lichens in a changing environment*. Oxford, UK: Oxford University Press, 362–380.
- Sierra AM, Vanderpoorten A, Gradstein SR, Pereira MR, Bastos CJP, Zartman CE. 2018. Bryophytes of Jaú National Park (Amazonas, Brazil): estimating species detectability and richness in a lowland Amazonian megareserve. *The Bryologist* 121: 571–588.
- Smith BT, McCormack JE, Cuervo AM, Hickerson MJ, Aleixo A, Cadena CD, Pérez-Emán J, Burney CW, Xie X, Harvey MG *et al.* 2014. The drivers of tropical speciation. *Nature* 515: 406–409.
- Snäll T, Fogelqvist J, Ribeiro PJ, Lascoux M. 2004. Spatial genetic structure in two congeneric epiphytes with different dispersal strategies analysed by three different methods. *Molecular Ecology* 13: 2109–2119.
- Sonah H, Bastien M, Iquiri E, Tardivel A, Légaré G, Boyle B, Normandeau E, Laroche J, Larose S, Jean M *et al.* 2013. An improved Genotyping by Sequencing (GBS) approach offering increased versatility and efficiency of SNP discovery and genotyping. *PLoS ONE* 8: e54603.
- Sujji PS, Martins K, de Oliveira Wadt LH, Renno Azevedo VC, Solferini VN. 2015. Genetic structure of *Bertholletia excelsa* populations from the Amazon at different spatial scales. *Conservation Genetics* 16: 955–964.
- Sundberg S. 2005. Larger capsules enhance short-range spore dispersal in *Sphagnum*, but what happens further away? *Oikos* 108: 115–124.
- Szövényi P, Sundberg S, Shaw AJ. 2012. Long-distance dispersal and genetic structure of natural populations: an assessment of the inverse isolation hypothesis in peat mosses. *Molecular Ecology* 21: 5461–5472.
- Vanderpoorten A, Patiño J, Désamoré A, Laenen B, Gorski P, Papp B, Hola E, Korpelainen H, Hardy OJ. 2019. To what extent are bryophytes efficient dispersers? *Journal of Ecology* 107: 2149–2154.
- Vekemans X, Hardy OJ. 2004. New insights from fine-scale spatial genetic structure analyses in plant populations. *Molecular Ecology* 13: 921–935.
- Wallace AR. 1852. On the monkeys of the Amazon. *Proceedings of the Zoological Society of London* 20: 107–110.
- Wang IJ, Bradburd GS. 2014. Isolation by environment. *Molecular Ecology* 23: 5649–5662.
- Zartman CE, Nascimento HEM. 2006. Are habitat tracking metacommunities dispersal limited? Inferences from abundance-occupancy patterns of epiphylls in Amazonian forest fragments. *Biological Conservation* 127: 46–54.
- Zartman CE, Nascimento HEM, Cangani KG, Alvarenga LDP, Snäll T. 2012. Fine-scale changes in connectivity affect the metapopulation dynamics of a bryophyte confined to ephemeral patches. *Journal of Ecology* 100: 980–986.
- Zartman CE, Shaw AJ. 2006. Metapopulation extinction thresholds in rain forest remnants. *American Naturalist* 167: 177–189.

Supporting Information

Additional Supporting Information may be found online in the Supporting Information section at the end of the article.

Fig. S1 Principal component analysis of posterior genotype probabilities based on RAD-seq data in 10 bryophyte species in central Amazonia.

Table S1 Voucher information and Sequence Read Archive (SRA) biosample accession numbers.

Table S2 Results of isolation-by-distance tests for three Amazonian bryophyte species based on SNP data after random sub-sampling of 100 SNPs.

Please note: Wiley Blackwell are not responsible for the content or functionality of any Supporting Information supplied by the authors. Any queries (other than missing material) should be directed to the *New Phytologist* Central Office.